Evidence for triggering of the Vogtland swarms 2000 by pore pressure diffusion

M. Parotidis,[1] S. A. Shapiro, and E. Rothert
Geophysics Department, Freie Universitaet Berlin, Berlin, Germany

Received 28 June 2004; revised 27 October 2004; accepted 26 January 2005; published 19 April 2005.

[1] Seismicity triggered by fluid injection in boreholes usually has certain typical spatiotemporal characteristics. These characteristics can be partly recognized as signatures, when pore pressure diffusion is the dominant triggering mechanism. Starting from these diffusion-typical signatures of man-made earthquakes, we seek analogous patterns for the earthquakes in Vogtland/NW Bohemia (VB) at the German/Czech border region in central Europe. VB is characterized by recurring intraplate earthquake swarms with magnitudes up to M_L 4.5. There is strong geophysical evidence that the seismic events are correlated to fluid-related processes in the crust. This study aims to investigate the possible role of fluids in VB. We test the hypothesis that ascending magmatic fluids trigger earthquakes by the mechanism of pore pressure diffusion (i.e., relaxation). This triggering process is mainly controlled by two physical fields, the hydraulic diffusivity and the seismic criticality (i.e., critical pore pressure value leading to failure; stable locations are characterized by higher critical pressures), both heterogeneously distributed in rocks. The results of the analysis of the year 2000 VB earthquake swarm data support this concept. We were able to recognize diffusive signatures and to obtain scalar estimates of hydraulic diffusivities with values between 0.3 and 10 m^2/s for the seismically active region. Using a numerical model, where spatially correlated diffusivity and criticality patches (where patches with higher diffusivity are assumed to be less stable) are considered, we successfully simulate a general seismicity pattern of the swarms 2000, including the spatiotemporal clustering of events and the migration of seismic activity.

Citation: Parotidis, M., S. A. Shapiro, and E. Rothert (2005), Evidence for triggering of the Vogtland swarms 2000 by pore pressure diffusion, *J. Geophys. Res.*, *110*, B05S10, doi:10.1029/2004JB003267.

1. Introduction

[2] Earthquake swarms are seismic sequences with no dominant magnitude, i.e., no main shock [*Lay and Wallace*, 1995]. In nature they often occur in volcanic regions, e.g., at the Somma-Vesuvius volcano in Italy [*Saccorotti et al.*, 2002], but also elsewhere, e.g., in the area of the Vosges Massif in France [*Audin et al.*, 2002], the recurrent earthquakes at Parkfield in central California [*Johnson and McEvilly*, 1995], the 1989 Dobi earthquake sequence of central Afar [*Noir et al.*, 1997], and in Vogtland/NW Bohemia (VB) covering the northwestern part of the Bohemian Massif [*Parotidis et al.*, 2003] (Figure 1). Common to all the above cases is the assumption that fluid flow is a possible triggering mechanism.

[3] On the other hand, by hydraulic fracturing experiments the induced seismicity shows certain spatiotemporal characteristics, which can be sometimes recognized as signatures for the triggering mechanism of pore pressure diffusion. *Shapiro et al.* [1997] presented an approach for describing diffusive characteristics of the pore pressure relaxation process using fluid-injection-triggered earthquakes. This concept has been further developed [*Shapiro*, 2000; *Shapiro et al.*, 2002; *Parotidis et al.*, 2004; *Parotidis and Shapiro*, 2004] and will be used here for the earthquake swarms 2000 in Vogtland/NW Bohemia (VB).

[4] After *Spicak and Horalek* [2001] many earthquake swarm regions are characterized by Quaternary volcanism, indicating that ascending magmatic fluids trigger earthquakes. These authors also suggest magmatic fluids as triggering mechanism in VB by stressing the similarity between the fault plane solutions for the earthquake swarms in VB and at the KTB borehole, ~50 km from VB, where fluid injections were carried out [*Zoback and Harjes*, 1997; *Rothert et al.*, 2003] (Figure 1).

[5] In this study the following hypothesis will be tested: The earthquake swarms in VB are triggered by ascending magmatic fluids, which change effective stresses by pore pressure perturbations. These approximately propagate according to the uncoupled pore pressure diffusion equation (see section 2.1). The spatiotemporal pattern of the seismic activity depends mainly on the spatial distribution of two physical fields, the hydraulic diffusivity $D(r)$ and the seismic criticality $C(r)$, i.e., critical pore pressure value leading to failure for a point r (a smaller $C(r)$ means a

[1]Now at GeoMechanics International, Inc., Mainz, Germany.

0148-0227/05/2004JB003267$09.00

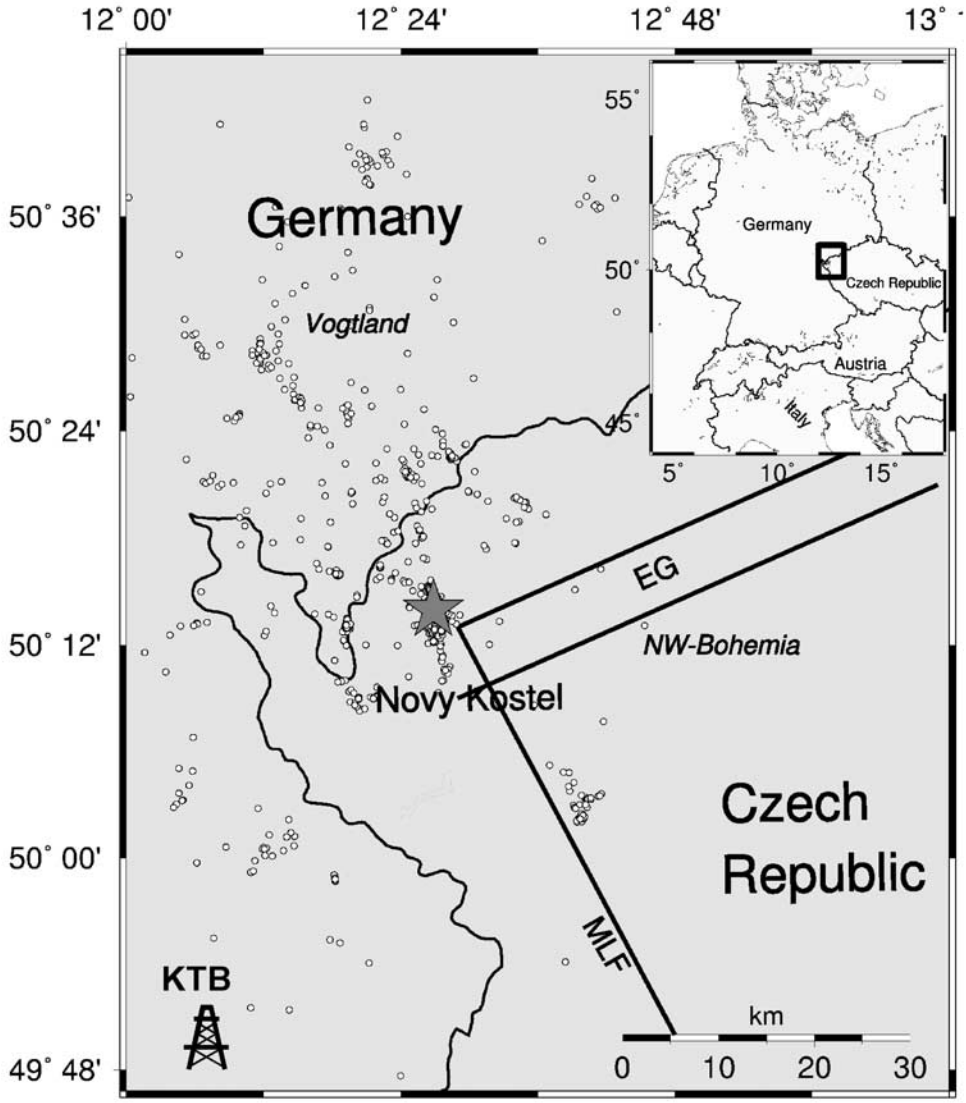

Figure 1. Map of Vogtland/NW Bohemia (VB). Circles denote earthquakes that occurred during 1994 and 2000 [see also *Fischer*, 2003; *Fischer and Horalek*, 2003]. The main epicentral region Novy Kostel (star) is ~50 km away of the German deep drilling site KTB (derrick). The straight lines symbolize the Eger graben (EG) and the Marianske Lazne fault zone (MLF).

more critical medium). Criticality can also be understood as a characteristic of the strength of the preexisting and prestressed cracks. *Wiprut and Zoback* [2000] used instead of criticality the term critical pressure perturbation, i.e., the pore pressure change that results in failure after the Mohr-Coulomb criterion [e.g., see *Jaeger*, 1972; *Jaeger and Cook*, 1976]. We test our hypothesis by (1) analyzing the data of the earthquake swarms in VB during the year 2000 and (2) simulating the seismicity pattern using a numerical model. Both the data analysis and the numerical simulations support the hypothesis formulated above.

2. Triggering Mechanism of Pore Pressure Diffusion

2.1. Poroelastic Diffusion Equation

[6] The time-dependent interaction of fluid flow and rock deformation is described by the theory of poroelasticity, which is based on Biot's equations [*Biot*, 1962]. One governing equation of linear poroelasticity is the following inhomogeneous diffusion equation for pore pressure p:

$$\frac{B}{3}\frac{\partial \sigma_{kk}}{\partial t} + \frac{\partial p}{\partial t} = \frac{k}{\mu S_\sigma} \cdot \nabla^2 p, \tag{1}$$

with B the Skempton's coefficient, $\sigma_{kk} = \sigma_{11} + \sigma_{22} + \sigma_{33}$ the mean stress, k the permeability, μ the viscosity of the fluid, S_σ the unconstrained specific storage coefficient, and t the time [*Wang*, 2000]. For an irrotational displacement field, assumed here to be approximately valid for fluid injections, equation (1) is mathematically uncoupled from the mechanical equilibrium equations, i.e., pore pressure perturbations propagate independently of stress changes:

$$\frac{\partial p}{\partial t} = D \cdot \nabla^2 p, \tag{2}$$

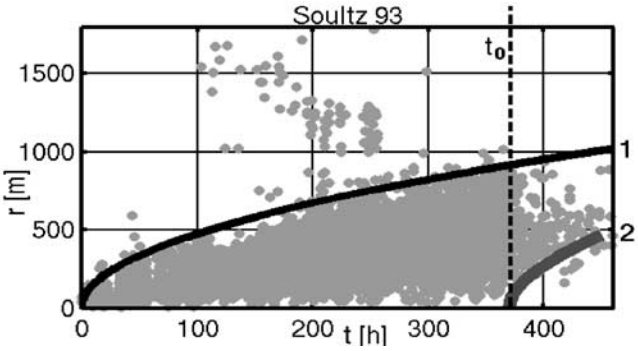

Figure 2. Plot of *r-t* for the Hot Dry Rock experiment in Soultz, France, 1993 [*Dyer et al.*, 1994; *Audigane et al.*, 2002]. *Shapiro et al.* [1999] estimated a diffusivity D = 0.05 m^2/s by applying the parabolic envelope signature (curve 1). *Parotidis et al.* [2004] confirmed this estimation by using the back front (curve 2) for fitting the data with the same diffusivity. Time t_0 = 370 hours corresponds to the end of fluid injection. Events above curve 1 (especially between 100 and 300 hours) may be due to hydraulic heterogeneities (for more details, see *Shapiro et al.* [1999] and *Parotidis et al.* [2004]).

with D the hydraulic diffusivity. The hydraulic diffusivity of the crust is generally estimated to be between 10^{-4} and 10 m^2/s [*Talwani and Acree*, 1984; *Kuempel*, 1991; *Wang*, 2000; *Scholz*, 2002]. In equation (2) the medium is assumed to be homogeneous and isotropic regarding elastic and hydraulic properties. The permeability k is related to the diffusivity by $D = k/(\mu S)$, where S is the uniaxial specific storage coefficient [*Wang*, 2000].

[7] Besides for borehole fluid injections, pore pressure diffusion (described by either the coupled or uncoupled equations) as triggering mechanism has been proposed for various case studies: e.g., for reservoir (large artificial lakes) induced seismicity [*Howells*, 1974; *Talwani*, 2000], for water table changes in large basins connected with microseismicity [*Costain and Bollinger*, 1991; *Lee and Wolf*, 1998], for volcanic seismicity in Italy [*Saccorotti et al.*, 2002], and for aftershocks of large earthquakes [*Nur and Booker*, 1972; *Bosl and Nur*, 2002; *Jonsson et al.*, 2003; *Shapiro et al.*, 2003; *Miller et al.*, 2004; *Koerner et al.*, 2004].

[8] In the following two signatures of the pore pressure diffusion triggering mechanism are presented: the parabolic envelope and the back front. These signatures are introduced on the base of the uncoupled equation (2).

2.2. Parabolic Envelope Signature

[9] *Shapiro et al.* [1997, 2003] and *Shapiro* [2000] developed a method, based on the uncoupled diffusion equation, initially for describing pore pressure perturbations caused by fluid injections into a borehole. They solved equation (2) for a step function point pore pressure source in a homogeneous isotropic saturated poroelastic medium, and estimated the distance r of the propagating front of significant pore pressure perturbations from the source, i.e., the injection point, with

$$r = \sqrt{4\pi D t}. \tag{3}$$

Equation (3) describes a parabola in an *r-t* plot. Such a parabola will be used in this study as a signature for detecting earthquake swarms triggered by pore pressure diffusion. Figure 2 shows a case study where this signature is applied.

2.3. Back Front Signature

[10] By fluid injections earthquakes are triggered during and after injection. The seismic activity after the end of injection may persist over hours and even days; see, e.g., the Hot Dry Rock experiments in Fenton Hill, New Mexico [*Fehler et al.*, 1998; *House*, 1987], and Soultz, France [*Dyer et al.*, 1994; *Audigane et al.*, 2002]. In order to explain this phenomenon we consider the pore pressure distribution due to a boxcar pressure source of duration t_0 (Figure 3) located at the origin of the coordinate system.

[11] The three-dimensional (3-D) solution of equation (2) for time $t \le t_0$ gives the pore pressure distribution $p_b(r, t)$ during injection; r is the distance from the injection point source of strength q (note, that q has physical units of power):

$$p_b(r,t) = \frac{q}{4\pi D r}\,\mathrm{erfc}\left(\frac{r}{\sqrt{4Dt}}\right), \tag{4}$$

with D the hydraulic diffusivity, and the so-called error function erf [e.g., see *Carslaw and Jaeger*, 1959]:

$$\mathrm{erfc}(x) = 1 - \mathrm{erf}(x) = 1 - \frac{2}{\sqrt{\pi}}\int_x^\infty \exp\left(-\xi^2\right)d\xi. \tag{5}$$

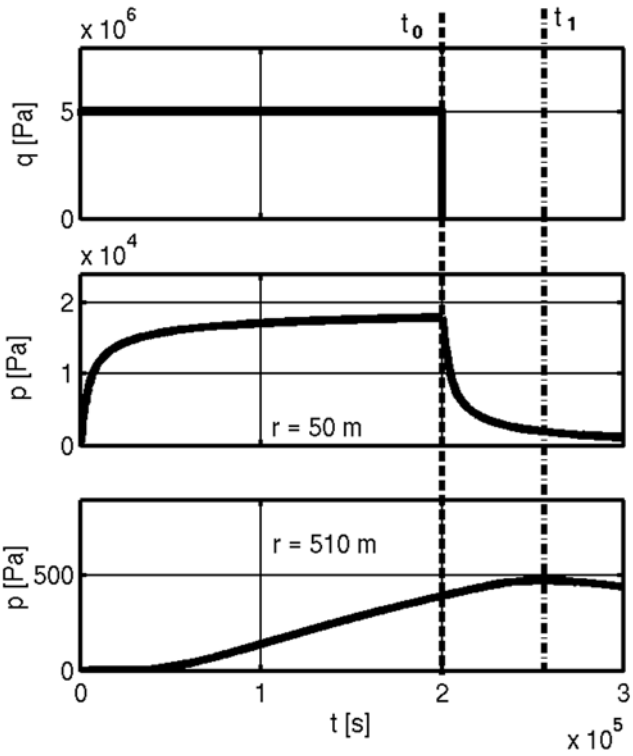

Figure 3. Distribution of pore pressure p (top) for a boxcar point pressure source q = 5 MPa, and of duration t_0 = 2×10^5 s, for points at distances (middle) r = 50 m and (bottom) r = 510 m from the injection point. The more distant a point from the source, the later the maximum pressure reached at time $t_1 > t_0$, i.e., after the end of fluid injection.

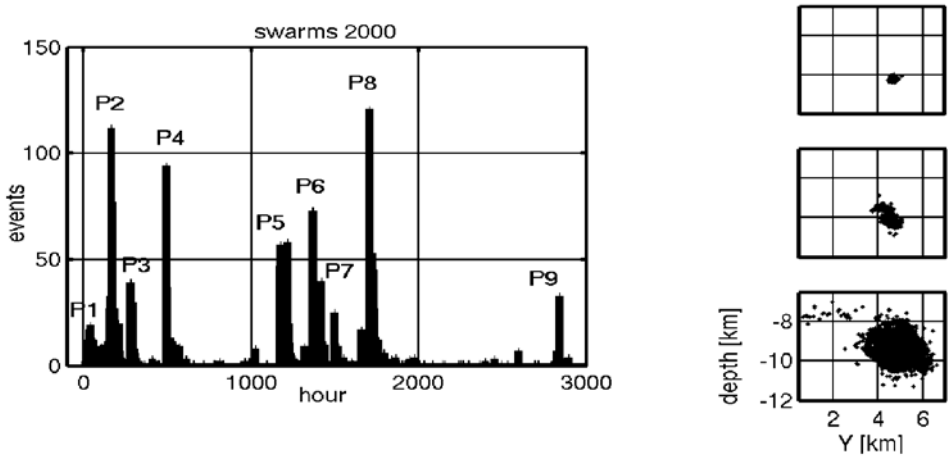

Figure 4. (left) Events versus time plot for the swarms 2000 in VB. The first event occurred on 28 August and the last on 26 December. The hours are calculated with reference to 28 August and time 0000. *Fischer* [2003] defined nine swarms, labeled P1 to P9. (right) Spatial evolution of earthquake swarms in N-S component (Y) and depth for (top) the beginning (with 50 events), (middle) an advanced state (with 600 events), and (bottom) the end of seismic activity (with 4400 events). This plot clearly shows that the seismic activity started in a narrow area (Figure 4, right, top) and later extended farther away (Figure 4, right, middle and bottom), thus explaining our assumption of a point pressure source that initiated the whole seismic process. The events in the upper left corner of Figure 4 (right, bottom) belong to swarm P9, the last triggered sequence.

For $t > t_0$, equation (6) is applied for the pore pressure $p_a(r, t)$ after the end of injection:

$$p_a(r,t) = \frac{q}{4\pi Dr}\left[\operatorname{erfc}\left(\frac{r}{\sqrt{4Dt}}\right) - \operatorname{erfc}\left(\frac{r}{\sqrt{4D(t-t_0)}}\right)\right]. \quad (6)$$

Assuming that for a given location events may be triggered only as long as pore pressure is increasing, would result in the absence of seismic activity after time t_1 at locations r where the maximum pressure is reached at this time $t_1(r)$ (see Figure 3). Depending on distance and time, this end of seismic activity should correspond to the solution of the equation where the pore pressure reaches its maximum, and therefore the time derivative of pore pressure after t_0, i.e., equation (6), equals zero:

$$\frac{\partial p_a}{\partial t} = \frac{q}{8(\pi D)^{3/2}}\left[\frac{\exp\left(-\frac{1}{4}\frac{r^2}{Dt}\right)}{t^{3/2}} - \frac{\exp\left(-\frac{1}{4}\frac{r^2}{D(t-t_0)}\right)}{(t-t_0)^{3/2}}\right] = 0. \quad (7)$$

The solutions for t in equation (7) give for every distance r the times $t_1(r)$ when the maximum pore pressure is reached. These solutions can be represented in an r-t plot by solving equation (7) for $r(t)$, resulting in the 3-D back front equation:

$$r = \sqrt{6Dt\left(\frac{t}{t_0} - 1\right)\ln\left(\frac{t}{t-t_0}\right)}. \quad (8)$$

Equation (8) describes a region of seismic quiescence developing after the end of injection. The corresponding 2-D equation is identical to equation (8) but for the factor 6, which must be replaced by 4. Figure 2 shows both the parabolic envelope and the back front signatures for real data of a fluid injection experiment. These signatures will be used in the following for indicating diffusive processes (and thus allowing diffusivity estimations) for the earthquake swarms in VB.

3. Seismicity in Vogtland/NW Bohemia (VB)

[12] VB in central Europe (Figure 1, inset) is characterized by recurring earthquake swarms, known since the 16th century with magnitudes up to M_L 4.5. The region exhibits CO2-rich mineral springs, some hundreds gas vents in eight mofette fields, 0.2 to 0.5 Myr old Quaternary volcanoes, a complex tectonic environment dominated by the Eger graben, which is crossed nearly perpendicularly by the Marianske Lazne fault zone [*Fischer and Horalek*, 2003] (Figure 1). The whole epicentral region covers 60 × 50 km^2 and corresponds to a transition zone from CO_2-dominated fluids to N_2-dominated fluids at the periphery [*Weinlich et al.*, 1998]. After *Weinlich et al.* [1999] an active degassing magma body located in the upper mantle provides the CO_2.

[13] Since 1985/1986 the main swarm earthquake activity in VB is concentrated in the Novy Kostel area (Czech Republic) defining a volume of a few cubic kilometers. The last large earthquake swarms were registered during 2000 with ~10,000 events and magnitudes up to M_L 3.3 and will be analyzed in the following. The seismic activity of the VB swarms 2000 comprises nine swarms clustered in time, designated P1 to P9 (Figure 4, left). All swarms but P9 are clustered also in space, comprising a volume of ~3.0 × 0.6 × 2.5 km3 (N-S × E-W × depth) (Figure 4, right). *Fischer* [2003] localized ~4500 events with an accuracy of ±100 m horizontally and ±190 m vertically.

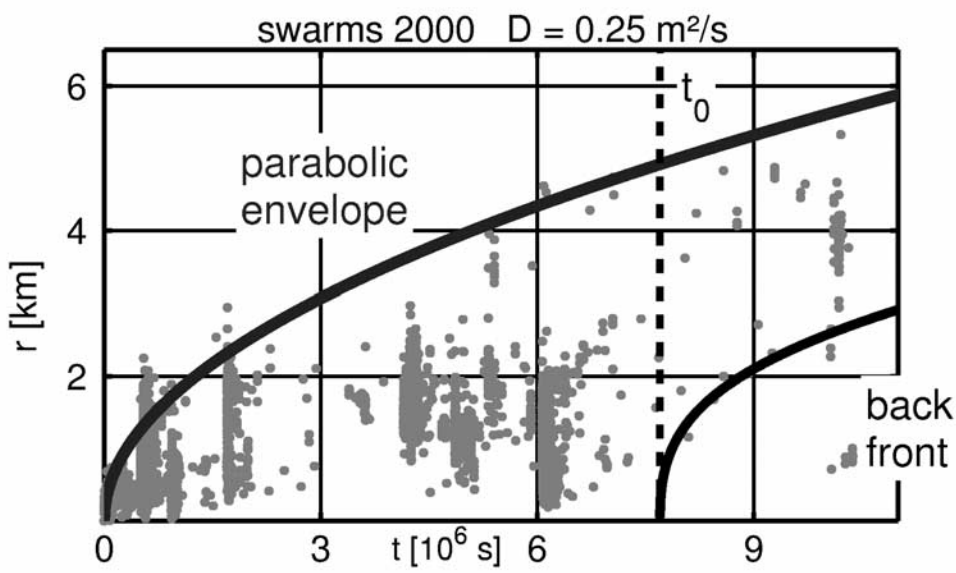

Figure 5. Plot of *r-t* for the VB swarms 2000 for the case of a single pore pressure source triggering all swarms. Parabolic envelope and back front are fitted to the data for $D = 0.25$ m^2/s, and $t_0 = 7.8 \times 10^6$ s. This complex seismicity pattern is mainly characterized by grouped events (swarms) with a strong temporal clustering, meaning events triggered in relatively short times over larger distances.

[14] The idea that ascending fluids trigger earthquakes in VB is not new. *Kämpf et al.* [1989] proposed a seismohydrological effect for VB, meaning chemical changes of the groundwater due to seismic activity. *Weise et al.* [2001], after examining the gas composition and its relation to seismic activity in VB, conclude that the seismicity is very probably triggered by fluids. *Horalek et al.* [2001], *Vavryzuk* [2001, 2002], *Hainzl and Fischer* [2002], *Babuska et al.* [2003], and *Klinge et al.* [2003] also consider fluids of importance for the seismic activity in VB. On the basis of chemical changes correlated to seismic activity, *Bräuer et al.* [2003] propose a fluid-driven mechanism for the swarms in VB.

4. Data Analysis

[15] For hydraulic fracturing experiments fluids are injected into boreholes. For VB we assume a similar scenario but turned upside down, where fluids, e.g., of magmatic origin, from deeper parts of the crust and/or mantle intrude to higher areas. So again we define a point pressure source. The aim of this analysis is to identify diffusive characteristics of the swarms 2000 in VB. *Fischer* [2003] defined nine swarms, designated P1 to P9, by estimating a waiting time (i.e., time between consecutive events with magnitudes above a defined value) for the events (Figure 4, left).

[16] First, we assume that a single pore pressure source triggered all swarms, and locate the injection point in the hypocenter of the first event. Relative to this point, distance r and occurrence time t are calculated for all events, in order to plot the corresponding *r-t* graph (Figure 5). For $D = 0.25$ m^2/s we fitted the data with a parabolic envelope and a back front. Nearly all events lie underneath the parabola and almost no earthquakes occur beyond the back front. Nevertheless, large parts of space under the parabola are without events; the events of the later swarms, between $3 \cdot 10^6$ s and $7 \cdot 10^6$ s, are clustered away of the envelope, and the events of the first swarms are partly above the parabola, thus rising two questions: (1) Could only one pressure source and the mechanism of pore pressure diffusion explain such a complex seismicity pattern. (2) If yes, what is the meaning of the estimated D. Generally, the two signatures deliver an effective upscaled diffusivity value for the seismically active region, presuming the single source assumption is valid; further, t_0 corresponds to the duration of the pore pressure perturbation triggering the earthquakes. Both the estimated diffusivity ($D = 0.25$ m^2/s) and the pore pressure perturbation duration time ($t_0 = 7.8 \cdot 10^6$ s) must be verified with a numerical model, which is presented in section 5.

[17] Second, we separately investigate each earthquake swarm for diffusive characteristics. Thus it is assumed that every swarm was triggered by its own injection point. These injection points are considered as secondary sources resulting from the single source, which initiated the whole triggering process. In order to exactly define the swarms the following criteria were used:

[18] 1. The temporal criterion is that all events of a swarm must be within a defined time window. The first event of the defined swarm provides the starting time of the assumed injection, i.e., a secondary source of the pore pressure perturbation.

[19] 2. The spatial criterion is that all events must lie within a defined volume. The location of the assumed secondary point source is defined as the centroid of the first 10 events of the swarm.

[20] Applying the above spatiotemporal criteria to the VB swarms 2000, 13 swarms were identified, designated nP1 to nP9 (including further subswarms, designated with a second digit). These are of shorter duration but with stronger clustering than the ones defined by *Fischer* [2003]. For

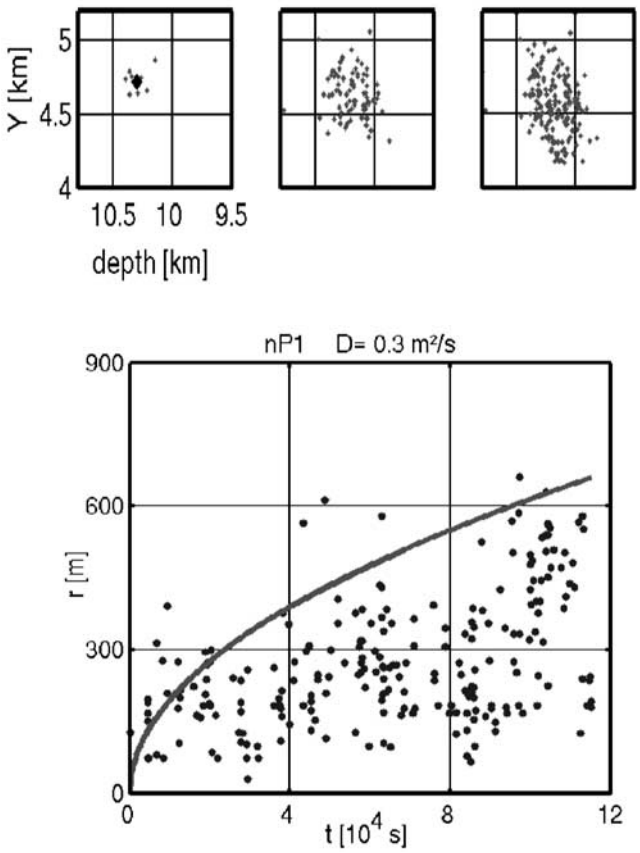

Figure 6. Earthquake swarm nP1. (top) Spatial evolution of the events in N-S component (Y axis) and depth. Snapshots are for 10, 100, and 220 events (from left to right). The diamond (left) denotes the hypothetical swarm's injection point. (bottom) Plot of *r*-*t* with parabolic envelope for $D = 0.3$ m^2/s.

example, Figures 6–8 show plots corresponding to the earthquake sequences nP1 and nP5. Swarm P5, after applying the above criteria, resulted in three earthquake swarms, labeled nP51 to nP53 (Figure 7). Further, we seek a parabolic envelope for each swarm in order to estimate a diffusivity characterizing the seismogenic zone of each swarm (e.g., Figure 6, bottom, and Figure 8), which was achieved for all but four swarms, namely nP4, nP6, nP71, and nP72 (see Table 1); the last three comprise too few

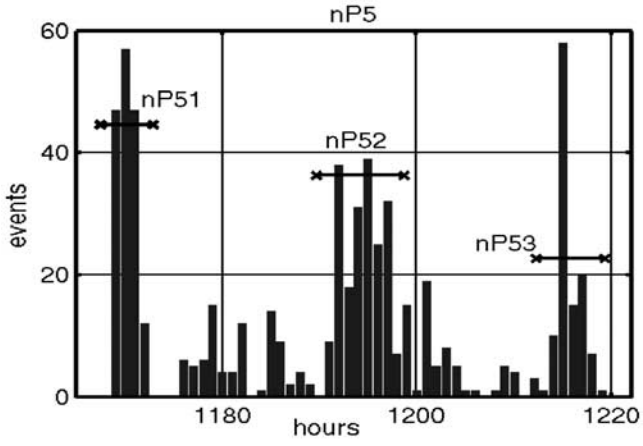

Figure 7. Events versus time plot for the P5 swarm, which shows that it actually comprises three swarms, labeled nP51 to nP53 (compare to Figure 4, left). Figure 8 shows the corresponding *r*-*t* plots.

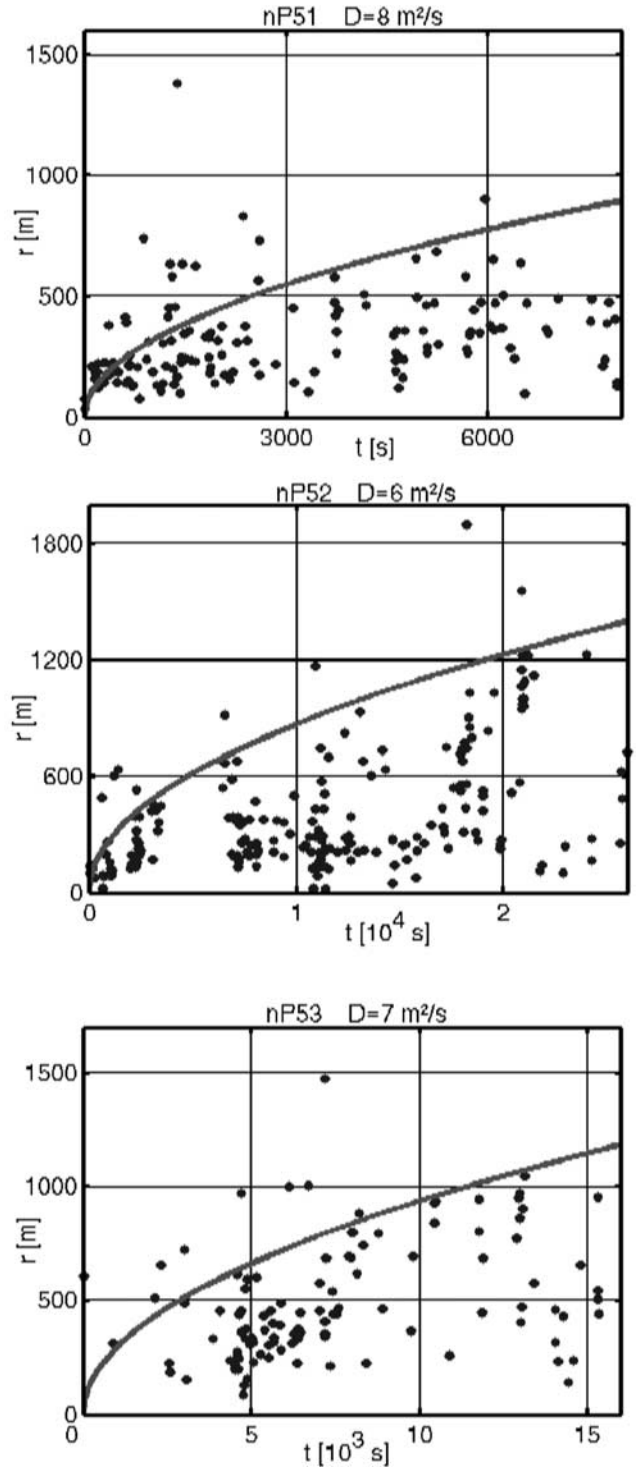

Figure 8. Plots of *r*-*t* with estimated hydraulic diffusivities *D* and corresponding parabolic envelopes for the swarms nP51 to nP53 (top to bottom), by assuming a (secondary) pore pressure source for each swarm.

Table 1. Estimated Diffusivities D for Earthquake Swarms 2000 in VB

Swarm	D, m^2/s
nP1	0.3
nP2	2.0
nP3	3.0
nP4	-
nP51	8.0
nP52	6.0
nP53	7.0
nP6	-
nP71	-
nP72	-
nP81	10.0
nP82	9.0
nP9	7.0

events (from 50 to 100) for defining an envelope. For swarm nP4, which although comprising a sufficient number of events, a gap of data in the seismic catalogue exists (T. Fischer, personal communication, 2003). The different values of diffusivity for each swarm indicate the existence of diffusivity patches. Also, these values correspond inversely to the waiting times estimated by *Fischer* [2003]; that was expected, as a higher value of diffusivity means larger pore pressure propagation velocities, i.e., shorter waiting times. Figure 9 shows the temporal migration of the seismic activity for all swarms.

[21] Summarizing, the main results of the data analysis of the swarms 2000 in VB are as follows: (1) We identified diffusive characteristics for the earthquake swarms by applying two signatures, the parabolic envelope (equation (3)) and the back front (equation (8)); (2) the assumption of a single pore pressure source triggering all events results in an *r-t* plot with strong temporal clustering of the events, and estimates for an effective diffusivity $D = 0.25$ m^2/s, and duration of a pressure perturbation $t_0 = 7.8 \times 10^6$ s (Figure 5); (3) by assuming that each swarm was triggered by its own pore pressure source, i.e., a secondary source, diffusivities with values between 0.3 and 10 m^2/s were estimated (Table 1), indicating the existence of hydraulic patches; and (4) the complex seismic activity evolution (Figure 9) can be simplified described as a counterclockwise migration of activity [see also *Fischer*, 2003].

5. Numerical Model

[22] *Rothert and Shapiro* [2003] proposed a methodology for modeling induced seismicity for various diffusivity/criticality fields, when pore pressure diffusion is the main triggering mechanism. Generally, diffusivity controls the pore pressure propagation; criticality defines if earthquakes will be triggered or not. The goal of the here presented numerical model is first to investigate the influence of heterogeneities on seismic signatures (section 5.1.); and second, to simulate the general seismicity pattern of the swarms 2000 in VB (section 5.2.) as found by the data analysis above (in section 4).

5.1. Diffusivity and Criticality Effects on Triggered Seismicity

[23] In this section, effects of heterogeneous spatial distributions of hydraulic diffusivity $D(r)$ and seismic criticality $C(r)$ on the seismicity pattern are modeled for events triggered by pore pressure diffusion. For a 2-D model we define a step function point pressure source in the middle of the investigation area. For simplicity, we consider a heterogeneity in the form of a rectangular patch (see Figure 10). Then we solve the diffusion equation with a finite element method (FEM) program. The result of each FEM calculation is the spatiotemporal distribution of pore pressure $p(r, t)$, which depends on the diffusivity field $D(r)$. Earthquakes are simulated by comparing the calculated pore pressures with the criticality at each discrete cell and for each time step; an event is triggered when the pressure in a cell exceeds its criticality. Then the corresponding *r-t* graph can be plotted. Figure 11 shows how a heterogeneity of $D(r)$ and/or $C(r)$ affects the *r-t* plot, or in other words, the seismic signature we can expect under certain conditions. The last plot shows that the spatially correlated high-diffusivity and highly critical (unstable) patches result in a temporal clustered seismic sequence, as observed in the data analysis for the different VB swarms 2000 (see Figure 5). This characteristic temporal clustering mirrors adjacent events triggered (due the highly critical patch) over larger distances in a relatively short time (due to the high-diffusivity patch).

5.2. Modeling of the VB Swarms 2000

[24] The aim of the following model is to simulate the general seismicity pattern of the swarms 2000 in VB, as found in section 4. We define a boxcar pore pressure source, of 1 MPa and duration $t_0 = 7.8 \cdot 10^6$ s, and place it at the bottom of five diffusivity patches, with diffusivities of 0.3, 3, 6, 10 and 8 m^2/s (according to the data analysis results), over a lower-diffusivity background with $D = 0.01$ m^2/s (Figure 12, top). Highly critical patches (randomly distributed with $C(r) < 1 \times 10^5$ Pa), spatially coinciding with the

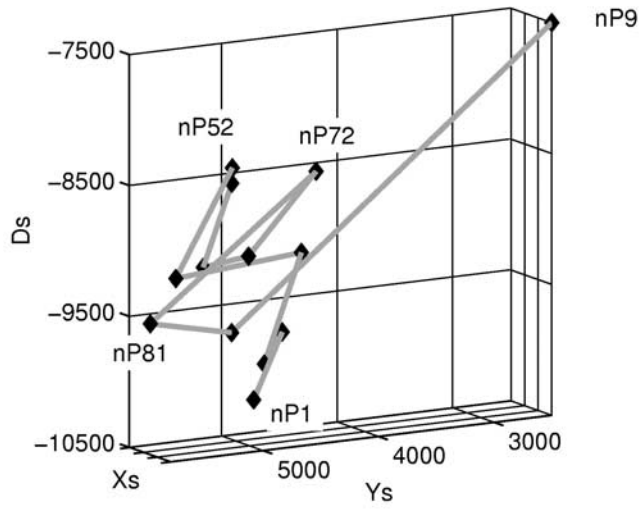

Figure 9. Three-dimensional plot with injection points (diamonds) of the 13 swarms of 2000 in VB. Injection points are connected according to occurrence time. The first triggered swarm was nP1, and the last was nP9. X_S, Y_S, and D_S denote the E-W, N-S, and depth coordinate components. Note that the extension of the swarm region along the X axis is only 600 m (in contrast to 3000 m along other axes). Therefore a 2-D approximation of the swarm geometry is a reasonable assumption.

Figure 10. (left) FEM solution of the diffusion equation for a point source. Contours give regions of same pore pressures and are circles around the source for an isotropic homogeneous diffusivity field. (middle) A diffusivity heterogeneity (rectangle, with a higher diffusivity than the background) which causes a distortion in the pressure distribution (here a faster pressure increase due to the high-diffusivity patch). (right) Criticality field with randomly distributed criticality values in the background and a highly critical patch (dark rectangle). Dark cells correspond to more critical regions, meaning that lower pressure changes can trigger earthquakes. So, bright cells represent more stable regions.

diffusivity patches, are defined over a randomly distributed stable background, with 10^5 Pa $< C(r) < 1.1 \times 10^6$ Pa (Figure 12, bottom). Thus the aim of the model is to simulate five earthquake swarms. Events are triggered in the cells where pore pressure exceeds criticality (Figure 13). Figure 14 shows the resulting *r-t* plot, which is the analogue of the data analysis result in Figure 5. The comparison of Figures 5 and 14 shows that (1) the model with a single pore pressure source successfully simulates the general spatio-temporal seismicity pattern of the swarms in VB; (2) for that, correlated criticality and diffusivity fields are required; (3) the estimated diffusivity D from the *r-t* plot gives an upscaled effective value representative for the whole seismically active region; this value is strongly influenced by high-diffusivity patches; (4) the back front beginning at time $t_0 = 7.8 \times 10^6$ s corresponds to the end of injection, that is

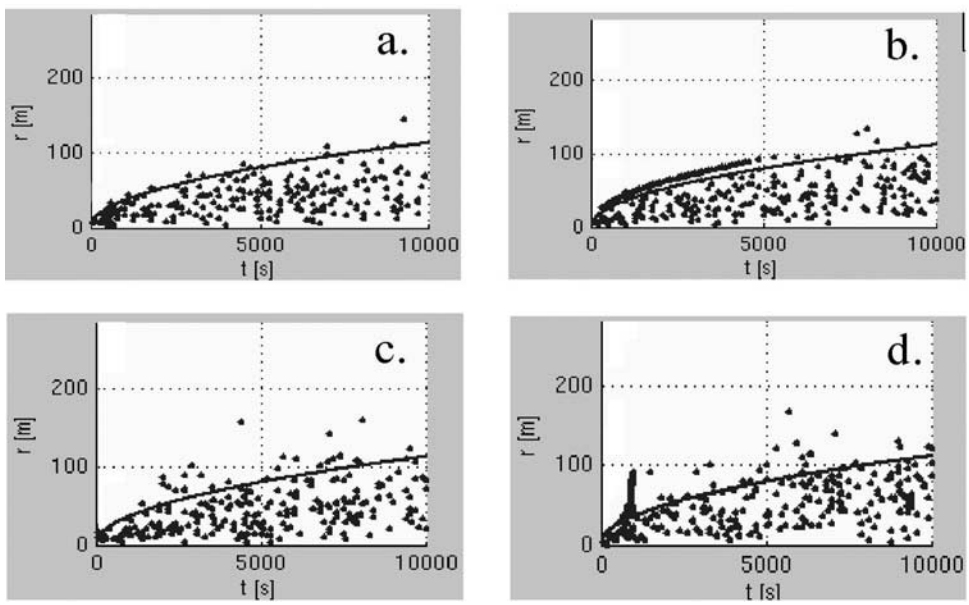

Figure 11. Plots of *r-t* with parabolic envelope for the input diffusivity value of numerical simulations for the following cases of diffusivity (D) and criticality (C) fields (see also Figure 10): (a) Homogeneous D and C. The majority of events are under the parabola for the input diffusivity value. (b) Homogeneous D and heterogeneous C (see Figure 10, right). Some events are clustered above and along the parabola. (c) Heterogeneous D (see Figure 10, middle) and statistically homogeneous C. More events than in case a. are above the parabola but show no clustering, as in Figure 11b. (d) Heterogeneous D and C. This is the only case resulting in a strongly temporal clustering of events (about $t = 1000$ s). Such event clusters are observed for the VB swarms 2000 in the analysis (see Figure 5). A highly critical patch allows for the spatial coherence of the seismic events (as in Figure 11b), but only in combination with a spatially correlated high-diffusivity patch the events are triggered very fast, i.e., in a relatively short time, thus presenting this characteristic temporal clustering.

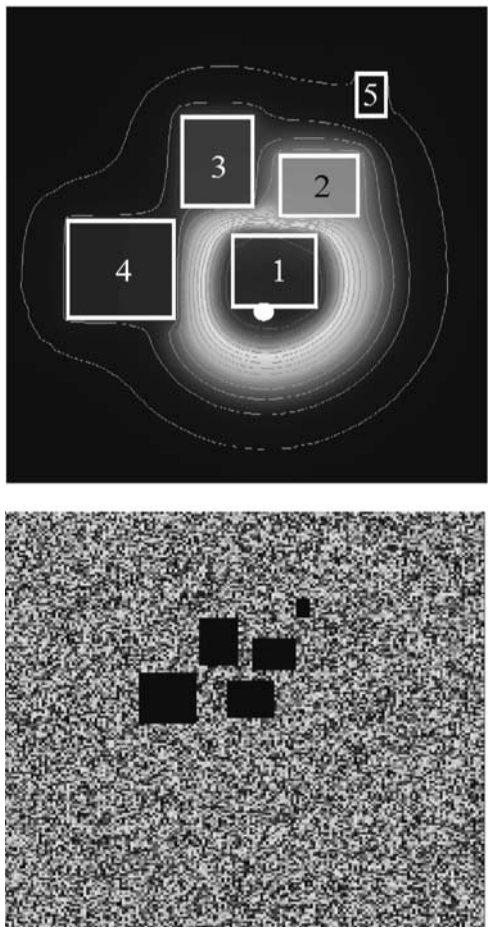

Figure 12. Two-dimensional numerical modeling of the VB swarms 2000. (top) Cutout (4×6 km^2) of the area of the FEM calculation. The single pressure source (circle) is placed at the bottom of five higher-diffusivity patches, with values of 0.3, 3, 6, 10, and 8 m^2/s for the patches with identities 1 to 5, respectively. The contours show regions of equal pressure values. (bottom) Criticality field with highly critical patches spatially identical with the diffusivity patches. The extension of the area of interest is 10×10 km^2.

the duration of pressure perturbations triggering the swarms 2000; and (5) the existence of the back front signature means that a part of the seismic events was triggered already after the end of a hypothetic process of injection of ascending fluids.

6. Discussion

[25] Here we discuss and summarize all assumptions and limitations of our analysis.

6.1. Fluids and Seismicity in VB

[26] The main goal of this study is to investigate the role of fluids in triggering earthquake swarms in VB. On the basis of geochemical analyses, *Kämpf et al.* [1989] and *Weise et al.* [2001] propose that seismic activity in VB is connected to chemical changes of water and gas of the region. On the basis of isotope observations before, during, and after a swarm, *Bräuer et al.* [2003] conclude that ascending magmatic fluids cause pore pressure changes and thus trigger the earthquakes. Correspondingly, we define a boxcar point source that causes the propagation of pressure perturbations in fluids filling the pore and fracture space in rocks. The fluid source is suggested by *Weinlich et al.* [1999] as a magmatic reservoir beneath the crossing of the Eger graben and the Marianske Lazne fault zone.

[27] *Bräuer et al.* [2003] estimated fluid transport velocities in VB between 50 and 400 m/day, from the hypocenter region to the surface. This large fluctuation agrees with the here estimated diffusivity values (characterizing the seismically active region) between 0.3 and 10 m^2/s (Table 1). We explained this by introducing diffusivity patches accounting for hydraulic heterogeneities. This idea is corroborated by *Bräuer et al.* [2003], as they describe the region in VB with differently permeable conduits and low-permeable rock units capping the hydraulic system. That corresponds well to our numerical modeling assumption of diffusivity patches over a less permeable background. The spatial clustering of seismic activity of the swarms 2000, and the spatiotemporal seismicity pattern (Figure 5) led us to assume highly critical

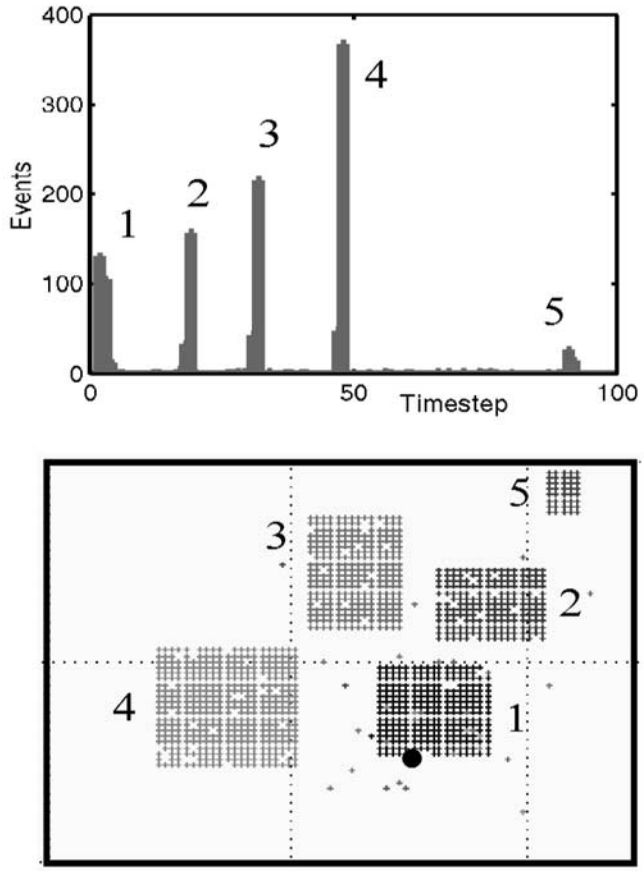

Figure 13. Two-dimensional numerical modeling of the VB swarms 2000. (top) Event versus time step plot, where 1 time step equals 7×10^4 s. The numbers correspond to the identities of the patches. (bottom) The 1238 triggered events (crosses), which clearly mirror the criticality patches (see Figure 12, bottom). The circle denotes the injection point. Comparing Figures 13 (top) and 13 (bottom), it can be seen that a counterclockwise migration of seismic activity occurred (swarms 1–4).

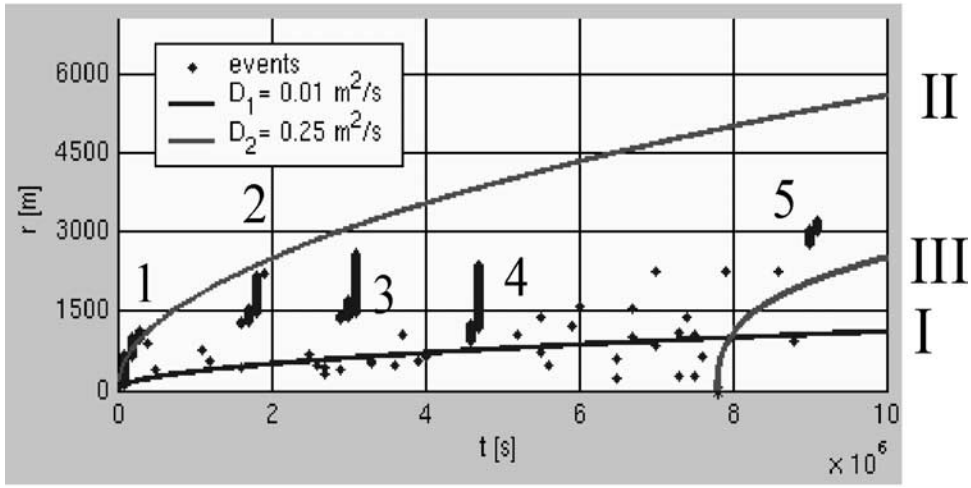

Figure 14. Two-dimensional numerical modeling of the VB swarms 2000; *r-t* plot with parabolic envelopes (curves I and II) for the diffusivities 0.01 and 0.25 m^2/s, respectively. The numbers next to the clusters denote the identity of each patch (see Figure 12, top). The characteristics of the seismicity pattern are the time delay of the triggering between the diffusivity patches (controlled by the diffusivity contrast of the patches to the background) and the vertical clustering of the events (controlled by the highly critical patches). The parabolic envelope (curve II) and the back front (curve III), both for $D = 0.25$ m^2/s, approximate the events as found by the swarm 2000 data analysis in Figure 5.

patches, too. These patches coincide with highly permeable patches.

[28] The hypocentral region of the swarms is mainly between 6 and 10 km depth. For this depth region the German seismic reflection profile DECORP3/MVE90, East, shows low-reflection structures, called white spots. These are interpreted as fluid enriched (i.e., porous) units [*Behr et al.*, 1994; *Bräuer et al.*, 2003]. Further information about the geologic and tectonic situation in VB is expected from the BOHEMA project [*Babuska et al.*, 2003].

[29] Also gravity changes are related to the seismic activity in VB. Observations indicate that gravity reaches a maximum before the highest seismicity rate occurs. As no topographical displacements and no groundwater table changes were observed, a possible explanation for the gravity anomalies could be a CO_2 flux increase before earthquakes are triggered [*Spicak et al.*, 1999; *Bräuer et al.*, 2003].

6.2. Data Analysis of the Swarms 2000 in VB

[30] For the data analysis in section 4 we assumed that a single point pressure source triggered all swarms. This is a simplifying approximation replacing a possibly in reality existing spatially constrained volume where significant pore pressure changes occur (similar to an open hole section by fluid injections). In order to produce the corresponding *r-t* plot (Figure 5) an injection point had to be defined. Therefore the first and deepest event was chosen, as the eventually nearest to an injection point of fluids coming from deeper regions. For each swarm we defined a secondary pressure source as a location, where a significant pressure perturbation has occurred (the centroid of the first 10 events).

[31] The assumption of secondary pressure sources is supported by the *r-t* plots for each swarm separately (Figure 6, bottom, and Figure 8), that allowed rough diffusivity estimates by applying the parabolic envelope signature. These estimates depend solely on the spatiotemporal seismicity pattern of each swarm. When the parabolic signature is applied then it is assumed that a step-function-like pressure perturbation triggered the events. The back front could not be applied to the individual swarms, as no corresponding signature could be observed. Nevertheless the whole VB swarm events could be approximated with a back front (Figure 5). This means that a boxcar like pore pressure perturbation, with duration $t_0 = 7.8 \times 10^6$ s, can explain earthquakes triggered after t_0. In other words the whole seismic activity of the VB swarms 2000 can be regarded as a coherent process. This interpretation is further supported by the presented numerical model (section 5.2., Figure 14). Perhaps the long duration of pressure perturbation is responsible too that no back front signatures could be observed for the different swarms, as all of them but P9 were triggered before t_0 (see Figure 5). We are not aware of any information or data that contradict our assumption of such a long pressure change (t_0 is about 3 months) in the crust and/or mantle. However, we know from volcanic areas that ascending magmatic fluids can significantly change pore pressures over even longer periods of time. Note that VB is characterized by Quaternary volcanism and magmatic fluids (see section 3).

[32] It is of course possible that the swarms were triggered by sources of independent fluid conduits, i.e., geologic structures, where pressure changes occurred at different times. Such a scenario is also possible to model but it would also require the determination of certain free parameters, e.g., location and duration of the different pressure sources. We believe that the here presented model was optimally determined in the sense of using a minimum of arbitrary input parameters.

6.3. Numerical Modeling

[33] The value of the model presented in section 5 is that it allowed us to use the derived results from the data analysis as input, in order to simulate principal features of seismicity pattern by defining a boxcar point pressure

source, and spatially correlated diffusivity and criticality patches. Thus the aim of the modeling was not to exactly reproduce the VB swarm 2000 data and so the analysis (Figure 5) and the modeling results (Figure 14) are not identical but similar: They show the same spatiotemporal characteristics but the model is restricted to the general seismicity pattern exemplified by the simulation of 5 and not 13 swarms. Further, the actual seismicity shows a more complex picture with regions partly reactivated, and a seismic activity migration path that only strongly simplified seems to be counterclockwise.

[34] The 2-D model is justified by the fact that the seismically active region shows a nearly planar character (Figure 9), indicating that it coincides with a fracture zone [*Fischer*, 2003] or a fault system. Thus the 3-D swarm data were approximated with a 2-D numerical model. This has no influence on the estimated diffusivities: The parabolic envelope is applied according to equation (3) for both the 2-D and 3-D case [*Shapiro et al.*, 1997, 1999, 2002]; the back front is described with (only slightly) different equations for 2-D and 3-D, as presented in section 2.3. It is reminded here that the diffusivity estimations with the above signatures deliver an order of magnitude estimates only [*Shapiro et al.*, 1997; *Shapiro*, 2000; *Parotidis et al.*, 2004]. Thus the difference of equations for 2-D and 3-D seismicity back front is insignificant here.

[35] The definition of 1 MPa as the magnitude of the injection point has no influence on the produced seismicity patterns, as this is compensated by the choice of the absolute value of the criticality field for the model. Anyway, the order of magnitude was proposed, as it agrees with borehole fluid injection experiments; for example, for the Hot Dry Rock experiment in Fenton Hill, New Mexico, 1983, the surface pressure was ~48 MPa [*Fehler et al.*, 1998], and for the KTB test the borehole pressure reached up to 50 MPa [*Zoback and Harjes*, 1997]. However, at points far from the borehole the pressure is much smaller.

6.4. Triggering Mechanism

[36] For the study presented here, pore pressure diffusion is considered as the main triggering mechanism in order to investigate the VB swarms 2000. This allowed us to apply the parabolic envelope and back front signatures for the analysis. The assumptions on which our data analysis is based were valid in the numerical model, but its results are similar and not identical to the real data, e.g., neither a complex migration of seismic activity nor partly overlapped swarms were simulated. So, there are differences between reality and analysis/modeling. We propose the following explanations:

[37] 1. The main triggering mechanism is pore pressure diffusion but more than one pressure sources are involved and/or have a more complex character than the step function/boxcar approximations used in this study.

[38] 2. Pore pressure diffusion is not the only triggering mechanism. Others, such as ΔCFS (change of Coulomb failure stress [see, e.g., *Beeler et al.*, 2000; *Kilb et al.*, 2002; *Scholz*, 2002]) and/or stress corrosion (subcritical crack growth in presence of fluids [see, e.g., *Atkinson and Meredith*, 1987; *Atkinson*, 1987]), may play an important role too. ΔCFS alone cannot explain the swarm activity as neither its static nor its dynamic components could explain the time delaying factor of the VB seismic activity. So, another triggering mechanism is needed. This could be pore pressure diffusion and/or stress corrosion. *Hainzl and Fischer* [2002] propose for the VB swarms 2000 a model where fluids initiated the swarm activity and later stress transfer and induced fluid flows are responsible for the earthquakes. Also *Hainzl and Ogata* [2004] presented an analysis based on statistical considerations for proposing a combination of mechanisms (ΔCFS and fluid action) for VB. These can be very reasonable models and further studies including different seismicity signatures are required.

7. Summary

[39] Vogtland/NW Bohemia (VB) in central Europe is a region characterized by natural recurring intraplate earthquake swarms. We hypothesize that ascending magmatic fluids trigger the earthquakes by causing pore pressure perturbations, which propagate according to the diffusion equation. This triggering process is mainly controlled by two physical fields, the hydraulic diffusivity and the seismic criticality of the rock. The results of the data analysis and modeling of the year 2000 swarms in VB support a concept, where pore pressure diffusion is the main triggering mechanism. The analyzed swarms show diffusive characteristics and render possible estimates of diffusivity, with values between 0.3 and 10 m^2/s, and an effective value of 0.25 m^2/s characterizing the whole seismically active region. Further the analysis allowed an estimate for the duration t_0 of the source of the pore pressure perturbation that triggered all events with $t_0 = 7.8 \times 10^6$ s. A 2-D numerical model was proposed, that successfully simulates principal features of the simplified seismicity pattern, by considering a boxcar pressure source of a duration which was shorter than the duration of the seismic activity. For that, the definition of spatially correlated diffusivity and highly critical patches is required. These patches could correspond to highly fractured and close to failure compartments of the fault zone region in VB, which allow enhanced fluid flow. In spite of the encouraging results, more investigations are necessary in order to account for the whole multitude of complex phenomena related to the earthquake swarms in VB.

[40] **Acknowledgment.** This work was funded by the German Research Foundation (Deutsche Forschungsgemeinschaft) under grant SH 55/3-1 and by SHELL International Exploration and Production B.V. Tomas Fischer provided the data and respective information.

References

Atkinson, B. (1987), Introduction to fracture mechanics and its geophysical applications, in *Fracture Mechanics of Rock*, edited by B. K. Atkinson, pp. 1–26, Springer, New York.

Atkinson, B., and P. Meredith (1987), The theory of subcritical crack growth with applications to minerals and rocks, in *Fracture Mechanics of Rock*, edited by B. K. Atkinson, pp. 111–166, Springer, New York.

Audigane, P., J.-J. Royer, and H. Kaieda (2002), Permeability characterization of the Soultz and Ogachi large-scale reservoir using induced microseismicity, *Geophysics*, *67*(1), 204–211.

Audin, L., J. Avouac, M. Flouzat, and J. Plantet (2002), Fluid-driven seismicity in a stable tectonic context: The Remiremont fault zone, Vosges, France, *Geophys. Res. Lett.*, *29*(6), 1091, doi:10.1029/2001GL012988.

Babuska, V., J. Plomerova, and BOHEMIA Working Group (2003), Seismic experiment searches for active magmatic source in deep lithosphere, central Europe, *Eos Trans. AGU*, *84*, 409 416–417.

Beeler, N., R. Simpson, S. Hickman, and D. Lockner (2000), Pore fluid pressure, apparent friction, and Coulomb failure, *J. Geophys. Res.*, *105*(B11), 25,533–25,542.

Behr, H. J., H. J. Dürbaum, and H. P. Bankwitz (1994), Crustal structure of the Saxothuringian Zone: Results of the deep seismic profile MVE-90 (East), *Z. Geol. Wiss.*, *22*, 647–769.

Biot, M. (1962), Mechanics of deformation and acoustic propagation in porous media, *J. Appl. Phys.*, *33*(4), 1482–1498.

Bosl, W. J., and A. Nur (2002), Aftershocks and pore fluid diffusion following the 1992 Landers earthquake, *J. Geophys. Res.*, *107*(B12), 2366, doi:10.1029/2001JB000155.

Bräuer, K., H. Kämpf, G. Strauch, and S. M. Weise (2003), Isotopic evidence ($^3He/^4He$, $^{13}CCO_2$) of fluid-triggered intraplate seismicity, *J. Geophys. Res.*, *108*(B2), 2070, doi:10.1029/2002JB002077.

Carslaw, H., and J. Jaeger (1959), *Conduction of Heat in Solids*, Oxford Univ. Press, New York.

Costain, J., and G. Bollinger (1991), Correlations between streamflow and intraplate seismicity in central Virginia, U.S.A., seismic zone: Evidence for possible climatic controls, *Tectonophysics*, *186*, 193–214.

Dyer, B., A. Juppe, R. H. Jones, T. Thomas, J. Willis-Richards, and P. Jaques (1994), Microseismic results from the European HDR Geothermal Project at Soultz-sous-Forets, Alsace, France, *Rep. IR03/24*, CSM Assoc.

Fehler, M., L. House, W. Philips, and R. Potter (1998), A method to allow temporal variation of velocity in travel-time tomography using micro-earthquakes induced during hydraulic fracturing, *Tectonophysics*, *289*, 189–201.

Fischer, T. (2003), The August-December 2000 earthquake swarm in NW Bohemia: The first results based on automatic processing of seismograms, *J. Geodyn.*, *35*, 59–81.

Fischer, T., and J. Horalek (2003), Space-time distribution of earthquake swarms in the principal focal zone of the NW Bohemia/Vogtland seismoactive region: Period 1985–2001, *J. Geodyn.*, *35*, 125–144.

Hainzl, S., and T. Fischer (2002), Indications for a successively triggered rupture growth underlying the 2000 earthquake swarm in Vogtland/NW Bohemia, *J. Geophys. Res.*, *107*(B12), 2338, doi:10.1029/2002JB001865.

Hainzl, S., and Y. Ogata (2004), Detecting fluid signals in seismicity data through statistical earthquake modeling, paper presented at XXIX General Assembly, Eur. Seismol. Comm., Potsdam, Germany.

Horalek, J., J. Sileny, T. Fischer, and J. Malek (2001), Source mechanisms and seismic models of the upper crust in the west Bohemia/Vogtland earthquake swarm region: Results obtained by the Webnet group, 26th General Assembly of the EGS, Eur. Geophys. Soc., Nice, France.

House, L. (1987), Locating microearthquakes induced by hydraulic fracturing in crystalline rocks, *Geophys. Res. Lett.*, *14*, 919–921.

Howells, D. (1974), The time for a significant change of pore pressure, *Eng. Geol.*, *8*, 135–138.

Jaeger, C. (1972), *Rock Mechanics and Engineering*, Cambridge Univ. Press, New York.

Jaeger, J. C., and N. G. W. Cook (1976), *Fundamentals of Rock Mechanics*, CRC Press, Boca Raton, Fla.

Johnson, P., and T. McEvilly (1995), Parkfield seismicity: Fluid-driven?, *J. Geophys. Res.*, *100*(B7), 12,937–12,950.

Jonsson, S., P. Segall, R. Pedersen, and G. Björnsson (2003), Post-earthquake ground movements correlated to pore-pressure transients, *Nature*, *424*, 179–183.

Kämpf, H., G. Strauch, P. Vogler, and W. Michler (1989), Hydrogeologic changes associated with the December 1985/January 1986 earthquake swarm activity in the Vogtland/NW Bohemia seismic area, *Z. Geol. Wiss.*, *17*, 685–689.

Kilb, D., J. Gomberg, and P. Bodin (2002), Aftershock triggering by complete Coulomb stress changes, *J. Geophys. Res.*, *107*(B4), 2060, doi:10.1029/2001JB000202.

Klinge, K., T. Plenefisch, and K. Stammler (2003), The earthquake swarm 2000 in the region Vogtland/NW-Bohemia—Earthquake recording at German stations and temporal distribution of events, *J. Geodyn.*, *35*, 83–96.

Koerner, A., E. Kissling, and S. A. Miller (2004), A model of deep crustal fluid flow following the M_w = 8.0 Antofagasta, Chile earthquake, *J. Geophys. Res.*, *109*, B06307, doi:10.1029/2003JB002816.

Kuempel, H. (1991), Poroelasticity: Parameters reviewed, *Geophys. J. Int.*, *105*, 783–799.

Lay, T., and T. Wallace (1995), *Modern Global Seismology*, Springer, New York.

Lee, M., and L. Wolf (1998), Analysis of fluid pressure propagation in heterogeneous rocks: Implications for hydrologically-induced earthquakes, *Geophys. Res. Lett.*, *25*, 2329–2332.

Miller, S. A., C. Collettini, L. Chiaraluce, M. Cocco, M. Barchi, and B. Kaus (2004), Aftershocks driven by a high-pressure CO_2 source at depth, *Nature*, *427*, 724–727.

Noir, J., E. Jacques, S. Bekri, P. M. Adler, P. Tapponnier, and G. C. P. King (1997), Fluid flow triggered migration of events in the 1989 Dobi earthquake sequence of central Afar, *Geophys. Res. Lett.*, *24*, 2335–2338.

Nur, A., and J. Booker (1972), Aftershocks caused by pore fluid flow?, *Science*, *175*, 885–887.

Parotidis, M., and S. A. Shapiro (2004), A statistical model for the seismicity rate of fluid-injection-induced earthquakes, *Geophys. Res. Lett.*, *31*, L17609, doi:10.1029/2004GL020421.

Parotidis, M., E. Rothert, and S. A. Shapiro (2003), Pore-pressure diffusion: A possible triggering mechanism for the earthquake swarms 2000 in Vogtland/NW-Bohemia, central Europe, *Geophys. Res. Lett.*, *30*(20), 2075, doi:10.1029/2003GL018110.

Parotidis, M., S. A. Shapiro, and E. Rothert (2004), Back front of seismicity induced after termination of borehole fluid injection, *Geophys. Res. Lett.*, *31*, L02612, doi:10.1029/2003GL018987.

Rothert, E., and S. A. Shapiro (2003), Microseismic monitoring of borehole fluid injections: Data modeling and inversion for hydraulic properties of rocks, *Geophysics*, *68*, 685–689.

Rothert, E., S. A. Shapiro, S. Buske, and M. Bohnhoff (2003), Mutual relationship between microseismicity and seismic reflectivity: Case study at the German Continental Deep Drilling Site (KTB), *Geophys. Res. Lett.*, *30*(17), 1893, doi:10.1029/2003GL017848.

Saccorotti, G., G. Ventura, and G. Vilardo (2002), Seismic swarms related to diffusive processes: The case of Somma-Vesuvius volcano, Italy, *Geophysics*, *67*, 199–203.

Scholz, C. H. (2002), *The Mechanics of Earthquakes and Faulting*, 2nd ed., Cambridge Univ. Press, New York.

Shapiro, S. A. (2000), An inversion for fluid transport properties of three-dimensionally heterogeneous rocks using induced microseismicity, *Geophys. J. Int.*, *143*, 931–936.

Shapiro, S., E. Huenges, and G. Borm (1997), Estimating the crust permeability from fluid-injection-induced seismic emission at the KTB site, *Geophys. J. Int.*, *131*, F15–F18.

Shapiro, S., P. Audigane, and J. Royer (1999), Large-scale in situ permeability tensor of rocks from induced microseismicity, *Geophys. J. Int.*, *137*, 207–213.

Shapiro, S. A., E. Rothert, V. Rath, and J. Rindschwentner (2002), Characterization of fluid transport properties of reservoirs using induced microseismicity, *Geophysics*, *67*, 212–220.

Shapiro, S. A., R. Patzig, E. Rothert, and J. Rindschwentner (2003), Triggering of seismicity by pore pressure perturbations: Permeability related signatures of the phenomenon, *Pure Appl. Geophys.*, *160*, 1051–1066.

Spicak, A., and J. Horalek (2001), Possible role of fluids in the process of earthquake swarm generation in the West Bohemia/Vogtland seismoactive region, *Tectonophysics*, *336*, 151–161.

Spicak, A., J. Mrlina, D. Jindra, and L. Mervart (1999), Monitoring of geodynamic activity in the West Bohemia seismoactive region between 1993–1996, *J. Geodyn.*, *27*, 119–132.

Talwani, P. (2000), Seismogenic properties of the crust inferred from recent studies of reservoir-induced seismicity—Application to Koyna, *Current Sci.*, *79*(9), 1327–1333.

Talwani, P., and S. Acree (1984), Pore pressure diffusion and the mechanism of reservoir-induced seismicitiy, *Pure Appl. Geophys.*, *122*, 947–965.

Vavrycuk, V. (2001), Inversion for parameters of tensile earthquakes, *J. Geophys. Res.*, *106*(B8), 16,339–16,355.

Vavrycuk, V. (2002), Non-double-couple earthquakes of 1997 January in West Bohemia, Czech Republic: Evidence of tensile faulting, *Geophys. J. Int.*, *149*, 364–373.

Wang, H. (2000), *Theory of Linear Poroelasticity*, Princeton Univ. Press, Princeton, N. J.

Weinlich, F. H., J. Tesar, S. M. Weise, K. Bräuer, and H. Kämpf (1998), Gas flux distribution in mineral springs and tectonic structure in the western Egger Rift, *J. Czech. Geol. Soc.*, *43*, 91–110.

Weinlich, F. H., K. Bräuer, H. Kämpf, G. Strauch, J. Tesar, and S. M. Weise (1999), An active subcontinental mantle volatile system in the western Eger Rift, central Europe: Gas flux, isotopic (He, C, and N) and compositional fingerprints, *Geochim. Cosmochim. Acta*, *63*, 3653–3671.

Weise, S. M., K. Bräuer, H. Kämpf, G. Strauch, and U. Koch (2001), Transport of mantle volatiles through the crust traced by seismically released fluids: A natural experiment in the earthquake swarm area Vogtland/NW Bohemia, central Europe, *Tectonophysics*, *336*, 137–150.

Wiprut, D., and M. D. Zoback (2000), Fault reactivation and fluid flow along a previously dormant normal fault in the northern North Sea, *Geology*, *28*(7), 595–598.

Zoback, M., and H. Harjes (1997), Injection-induced earthquakes and crustal stress at 9 km depth at the KTB deep drilling site, Germany, *J. Geophys. Res.*, *102*(B8), 18,477–18,491.

M. Parotidis, GeoMechanics International, Inc., Emmerich-Josef-Str. 5, D-55116 Mainz, Germany. (mparotidis@geomi.com)

E. Rothert and S. A. Shapiro, Geophysics Department, Freie Universitaet Berlin, Malteserstr. 74-100, Building D, D-12249 Berlin, Germany. (shapiro@geophysik.fu-berlin.de)